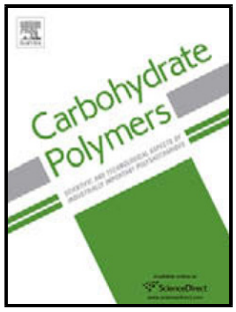

Title: Starch–zinc complex and its reinforcement effect on starch-based materials

Authors: Peng Liu, Ying Li, Xiaoqin Shang, Fengwei Xie

PII: S0144-8617(18)31367-5
DOI: https://doi.org/10.1016/j.carbpol.2018.11.034
Reference: CARP 14285

To appear in:

Received date: 5 July 2018
Revised date: 10 November 2018
Accepted date: 11 November 2018

Please cite this article as: Liu P, Li Y, Shang X, Xie F, Starch–zinc complex and its reinforcement effect on starch-based materials, *Carbohydrate Polymers* (2018), https://doi.org/10.1016/j.carbpol.2018.11.034

Starch–zinc complex and its reinforcement effect on starch-based materials

Peng Liu[a], Ying Li[a], Xiaoqin Shang[a,*], Fengwei Xie[b,c,d,**]

[a] *School of Chemistry and Chemical Engineering, Guangzhou University, Guangzhou 510006, China*

[b] *Institute of Advanced Study, University of Warwick, Coventry CV4 7HS, United Kingdom*

[c] *International Institute for Nanocomposites Manufacturing (IINM), WMG, University of Warwick, Coventry CV4 7AL, United Kingdom*

[d] *School of Chemical Engineering, The University of Queensland, Brisbane, Qld 4072, Australia*

[*] Corresponding author. *Email address:* hushanren@163.com (X. Shang);

[**] Corresponding author. *Email address:* f.xie@uq.edu.au; fwhsieh@gmail.com (F. Xie).

Graphical abstract

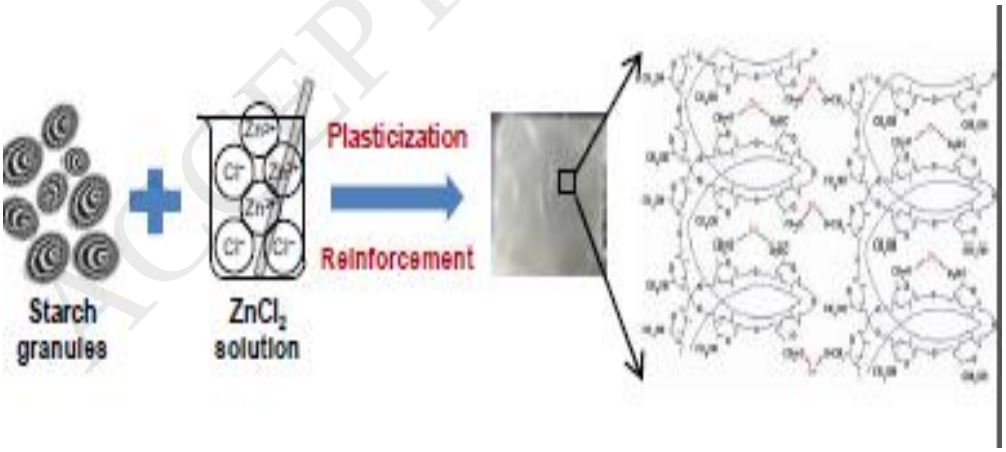

Highlights:

- $ZnCl_2$ solution showed an excellent plasticization effect on starch
- Higher $ZnCl_2$ content led to a larger size of starch-zinc complexes
- Higher $ZnCl_2$ content led to less shear-thinning of waxy corn starch/$ZnCl_2$ solution
- Starch-zinc complexes enhanced the mechanical properties of starch-based materials
- Shear further strengthened the mechanical properties of starch-based materials

Abstract:

In this work, we found that $ZnCl_2$ solution can not only be used as a plasticizer for starch but also provide a mechanical reinforcement effect to the resultant starch-based materials. By a one-step compression molding process, well-plasticized starch-based films could be obtained at 120 °C with a 15 wt.% $ZnCl_2$ solution. Both the tensile strength and elongation at break of the films increased with a rise in $ZnCl_2$ concentration, which demonstrates a mechanical reinforcement. This reinforcement could be mainly ascribed to the *in-situ* formed starch-zinc complexes and the enhanced starch molecular interactions. Moreover, if the processing method was changed into firstly mixing followed by compression molding, the tensile strength increased by more than three folds at no cost of the elongation at break. Regarding this, we propose that shear could further enhance the molecular interactions within the material. However, if the $ZnCl_2$ concentration was too high, the mechanical properties were then reduced irrespective of the processing protocol, which could be due to the weakened molecular interactions by $ZnCl_2$. Thus, we have demonstrated a new, simple method for preparing starch-based composite materials with enhanced mechanical properties, which could be potentially applied to many fields such as packaging, coating and biomedical materials.

Keywords:

Starch-based materials; reinforcement; plasticization; mechanical properties

Chemical compounds studied in this article:

Starch (PubChem CID: 24836924); Water (PubChem CID: 962); Zinc chloride (PubChem CID: 5727).

1 Introduction

Starch is a renewable resource that is abundant in nature (Xie, Pollet, Halley, & Avérous, 2013; Yang et al., 2016) and has been used in chemical, food, pharmaceutical and petroleum industries (Bie et al., 2013; Tang et al., 2015). Moreover, because of the environmental concerns and waste management, there has been ongoing research for replacing conventional non-biodegradable plastics with natural biopolymers such as starch (Iamareerat, Singh, Sadiq, & Anal, 2018; Nagy et al., 2017).

Unfortunately, starch has poor processability and starch-based materials usually display weak mechanical properties, which form the bottlenecks for their applications (Ali et al., 2018; Youssef & El-Sayed, 2018). To improve the processability of starch, many studies have been undertaken to find suitable plasticizers for starch, such as water, glycerol (Fazeli, Keley, & Biazar, 2018; Zuo, Gu, Tan, & Zhang, 2015), formamide (Zuo et al., 2015), urea (Correa, Carmona, Simão, Capparelli Mattoso, & Marconcini, 2017; Rychter et al., 2016; Zuo et al., 2015), poly(citrate glyceride) (Kang et al.,

2018), poly(trimellitic glyceride) (Zhang, Cheng, Lin, Zhou, & Zhu, 2018), ionic liquids (Liu & Jin, 2016; Xie et al., 2014; Zhang et al., 2016; Zhang et al., 2017) and eutectic solvents (Magdalena & Caisa, 2017). However, these plasticizers always have their respective disadvantages such as poor stability, low efficiency, high toxicity, and high costs. For example, while ionic liquids have been identified as an effective hydrogen-bonding breaker and an effective solvent for different natural polymers including starch (Wang, Gurau, & Rogers, 2012; Wilpiszewska & Spychaj, 2011; Zakrzewska, Bogel-Łukasik, & Bogel-Łukasik, 2010; Zhu et al., 2006), they are still quite expensive for polymer processing and their toxicity is still under investigation (Thuy Pham, Cho, & Yun, 2010). Thus, research has been ongoing for seeking suitable plasticizers.

On the other hand, to improve the mechanical properties of starch, various reinforcing agents have been investigated, such as cellulose nanofibers (Sheikhi & van de Ven, 2018), lignocellulosic fibers (Ibrahim, Mehanny, Darwish, & Farag, 2018), nanoclays (Bahruddin, Hendri, Rifaldi, Syaputra, & Rochaeni, 2018), ZnO nanoparticles (Ma, Zhu, Tian, & Wang, 2016; Nadanathangam, Sampath, Kathe, Varadarajan, & Virendra, 2006; Yu, Yang, Liu, & Ma, 2009), and crosslinked starch particles (Cao et al., 2010). However, the dramatically increased properties of the resultant starch nanocomposites were not always the case due to the poor dispersion of the nanofiller, and further chemical modification and processing strategies need to be sought to enhance the polymer-nanofiller interfacial interactions (Xie et al., 2013), which could potentially increase the overall costs.

Recent studies (Chen et al., 2017; Lin et al., 2016; Luo et al., 2013; Luo et al., 2016) have shown that zinc chloride solutions of certain concentrations could dissolve starch granules completely. The reasons for this is that Zn^{2+} ions can penetrate into the inner structure of starch granules, weaken the

intra- and intermolecular hydrogen bonds, and disrupt the crystalline regions, finally leading to the dissolution of starch. Specifically, there are 10 electrons on the 3*d* electronic orbit of Zn^{2+}, and by an *sp*3 hybridized effect, the 4*s* and 4*p* electronic orbits can form four *sp*3 hybrid orbits. In Zn^{2+} solutions, each *sp*3 hybrid orbit of Zn^{2+} can accept one pair of electrons on the oxygen atom of H_2O to generate a $[Zn(H_2O)_4]^{2+}$ complex (Lu & Shen, 2011; Xu, Chen, Rosswurm, Yao, & Janaswamy, 2016). Since this complex still has two positive charges in its outermost shell, it still has two 4*d* activated electronic orbits, which can accept one or two isolated charges on the oxygen atoms of starch hydroxyls and leading to an octahedral geometry (Fischer, Leipner, Thümmler, Brendler, & Peters, 2003; Leipner, Fischer, Brendler, & Voigt, 2000). Based on X-ray photoelectron spectroscopy (XPS) and ^{13}C cross-polarization/magic-angle spinning nuclear magnetic resonance (^{13}C CP/MAS NMR), Zn^{2+} has been found to be mainly coordinated to the oxygen atoms of the glucose unit 6-CH_2OH (Luo et al., 2013; Luo et al., 2016). In this way, it has been suggested that a "starch–zinc inclusion complex" forms in starch–$ZnCl_2$ aqueous solutions (Chen et al., 2017; Lin et al., 2016; Luo et al., 2013; Luo et al., 2016). On the other hand, there have been some reports on starch-based nanocomposites reinforced by ZnO nanoparticles (Ma et al., 2016; Nadanathangam et al., 2006). In these studies, the ZnO nanoparticles could be obtained by adjusting the pH of $ZnCl_2$ or $Zn(NO_3)_2$ aqueous solution by NaOH solution and could be stabilized by starch or carboxymethylcellulose. In contrast, we intended to develop a simple method to prepare starch-based materials with enhanced properties. Many studies (Ciesielski, Lii, Yen, & Tomasik, 2003; Kweon, Choi, Kim, & Lim, 2001; Para, 2004; Para, Karolczyk-Kostuch, & Fiedorowicz, 2004; Zhang & Chen, 2002) have demonstrated the interactions or complexation between starch and different metal ions. We

hypothesized that $ZnCl_2$ aqueous solutions can be used to plasticize starch and simultaneously provide a reinforcement effect by the *in-situ* formed starch-zinc complexes.

In this work, we first investigated the enlargement and stability of starch-zinc complexes in starch/$ZnCl_2$ solutions by ways of size distribution and reduced viscosity. Subsequently, the starch-based materials plasticized by $ZnCl_2$ solutions using industrially relevant melt processing techniques were prepared. The conformation of starch–zinc complexes is discussed and the plasticization and reinforcement effects of $ZnCl_2$ solutions for starch-based materials are demonstrated. We chose a high-amylose corn starch (Gelose 80) and waxy corn starch as model starches for our investigation. The amylose content is known to significantly influence the processability and material properties (Li et al., 2011; Liu, Yu, Xie, & Chen, 2006; Liu, Xie, Yu, Chen, & Li, 2009a; Liu et al., 2011; Wang et al., 2010; Xie, Halley, & Avérous, 2012). Besides, while previous studies have proposed amylose-zinc inclusion complexes, we intended to test if such complexation would occur between amylopectin and Zn^{2+} ion.

2 Materials and Methods

2.1 Materials

Waxy corn starch (about 1% amylose content) was supplied by Lihua Starch Industry Co., Ltd. Gelose 80 corn starch (G80) (about 80% amylose content, as determined by the manufacturer) was supplied by National Starch Pty Ltd. (Lane Cove, NSW 2066, Australia). Anhydrous zinc chloride

($ZnCl_2$) and ethanol (analytical grade) were purchased from Guangzhou Chemical Reagent Factory (Guangzhou, China). All solutions were prepared with distilled water.

2.2 Rheological study of starch/$ZnCl_2$ solutions

The rheological measurements were carried out on a rheometer (MCR 92, Anton Paar Company, Austria) with a 60-mm-diameter plate-plate geometry and a Peltier temperature control system. Silicone oil (DC 200, Sigma-Aldrich) was placed around the edge of the measuring cell to prevent the absorption of water from the environment. Silicone oil would hardly affect the experimental results as it is not miscible with polysaccharide solutions and has a relatively lower viscosity (9.5 mPa·s at 20 °C) (Liu & Budtova, 2013; Tajuddin, Xie, Nicholson, Liu, & Halley, 2011). The steady shear experiments were carried out with shear rate from 10 s^{-1} to 400 s^{-1} at 30 °C (as a typical temperature). The starch concentration of all the samples was set at 5 wt.% (dry weight). Four $ZnCl_2$ concentrations of 30%, 35%, 45% and 65% were used for waxy starch, and 45%, 50%, 60% and 65% for G80 starch (Chen et al., 2017). Here, 30% was the lowest $ZnCl_2$ concentration to dissolve waxy corn starch and 45% the lowest for G80 corn starch without precipitation (Lin et al., 2016). All the rheological tests were carried out at least twice to ensure the consistency of results.

The reduced viscosity is calculated using Eq. (1) below (Chen & Joslyn, 1967; Sahin & Sumnu, 2006):

$$\eta_{\mathrm{red}} = \frac{\eta/\eta_0 - 1}{c} \qquad (1)$$

where η_{red} is the reduced viscosity of samples in mL/g; η is the viscosity of starch/$ZnCl_2$ solutions in mPa·s; η_0 is the viscosity of $ZnCl_2$ solutions in mPa·s; and c is the concentration of starch, namely 5 wt.%.

2.3 Size distribution study of starch/$ZnCl_2$ solutions

The distributions of starch particle size in $ZnCl_2$ solutions were detected via dynamic light scattering (DLS) measurements using a Zetasizer machine (ZEN 3690, Malvern Instruments, UK). The light (k = 632.8 nm) from a solid-state He-Ne laser (22 mW) was used as the incident beam. The measurements were conducted at a scattering angle of 90° at a temperature of 25.0±0.1 °C. The results were analyzed via Malvern Zetasizer Software v7.11 (Wu et al., 2017; Zhong, Wyman, Yang, Wang, & Wu, 2016).

To prepare the solutions, anhydrous $ZnCl_2$ were added to a three-neck, round-bottom flask equipped with an electric stirrer to obtain $ZnCl_2$ solutions (30% $ZnCl_2$ concentration for waxy corn and 45% $ZnCl_2$ concentration for G80 corn starch). Then, the starch samples (1.0 wt.%, dry weight) were added to the solutions and stirred at 50 °C for 4 h. To prevent the possible degradation by shear force, a low revolution speed of 60 rpm was chosen. After dissolution, the starch/$ZnCl_2$ solution was homogenous and was a clear solution. The particles sizes in the solutions were detected immediately. After that, anhydrous $ZnCl_2$ was added into the waxy starch/$ZnCl_2$ solution to increase the $ZnCl_2$ concentration to 45%, 55%, and 60% systematically. The size distribution was detected for each $ZnCl_2$ concentration. For the G80/$ZnCl_2$ solution, the $ZnCl_2$ concentration was increased to 50%,

60%, and 65% stepwise. The pH values of solutions were mainly influenced by the concentration of $ZnCl_2$, with pH = 4.09 for 30 wt.% and pH = 0.67 for 65 wt.%.

2.4 Preparation of starch-based films

Table 1 shows the sample formulations for preparing starch-based films. First, $ZnCl_2$ solutions of different concentrations were prepared. Then, the solutions were added dropwise to starch powders (wet basis, containing 14.1 wt.% moisture content), accompanied by careful blending using a mortar and pestle to ensure an even distribution of the solution in starch. For all materials, the weight ratio between the starch powder and the solution was fixed to be 100:30 (wt./wt.). Starch-based films were prepared using either of the two processing methods, namely (1) only compression molding (CM) and (2) first mixing followed by compression molding (MC). Sample codes as "G-15/CM" were used in the following text, where "G" (or "W") means Gelose 80 corn starch (or waxy corn starch), "15" indicates the $ZnCl_2$ concentration of $ZnCl_2$ solution, and "CM" (or "MC") represents the processing method used. Films could not be successfully formed from samples formulated with $ZnCl_2$ solutions of even higher $ZnCl_2$ concentrations than the ones shown in **Table 1**.

Table 1. Sample formulations and crystallinity of starch-based films.

Sample	Starch content (g)	Water content (g)	$ZnCl_2$ content (g)	Crystallinity (%)
G-0/CM	100	30.00	0.00	16.8±0.6[a]
G-15/CM	100	25.50	4.50	15.6±0.4[a]
G-20/CM	100	24.00	6.00	8.5±0.2[b]

G-25/CM	100	22.50	7.50	8.2±0.4[b]
G-30/CM	100	21.00	9.00	7.2±0.3[b]
G-35/CM	100	19.50	10.50	5.1±0.4[c]
W-0/CM	100	30.00	0.00	22.1±0.8[a]
W-15/CM	100	25.50	4.50	17.0±0.6[b]
W-20/CM	100	24.00	6.00	15.3±0.7[b]
W-25/CM	100	22.50	7.50	11.9±0.4[b]
W-30/CM	100	21.00	9.00	14.0±0.4[b]
G-0/MC	100	30.00	0.00	18.0±0.4[a]
G-15/MC	100	25.50	4.50	12.1±0.2[b]
G-25/MC	100	22.50	7.50	11.5±0.5[b]
G-30/MC	100	21.00	9.00	9.2±0.2[c]
G-35/MC	100	19.50	10.50	7.5±0.2[d]
G-40/MC	100	18.00	12.00	6.2±0.3[d]
W-0/MC	100	35.00	0.00	21.7±0.7[a]
W-15/MC	100	25.50	4.50	13.6±0.4[b]
W-25/MC	100	22.50	7.50	10.9±0.3[c]
W-30/MC	100	21.00	9.00	9.9±0.6[c]
W-35/MC	100	19.50	10.50	8.8±0.4[d]
W-40/MC	100	18.00	12.00	8.8±0.3[d]

Superscripts with different letters in the same column indicate significant differences ($p \leq 0.05$).

For CM, a previously reported method (Xie et al., 2014; Xie et al., 2015; Zhang et al., 2016; Zhang et al., 2017) was followed. Specifically, the powder (25 g, dry weight) was carefully and equally spread over the molding area (15 cm × 15 cm = 225 cm^2) with poly(tetrafluoroethylene) (PTFE) glass fabrics located between the starch and the mold. For the subsequent compression molding, a flat sulfuration machine (Guangzhou Shunchuang Rubber Machinery Factory, Guangzhou, China) was used. It has two press areas with the upper one for hot press and the lower one maintained at room temperature for cooling. Each sample in the mold was first hot-pressed in the upper area at a temperature of 120 °C and a pressure of 10 MPa for 6 min, which was then

immediately moved to the lower area and pressed under 10 MPa for cooling for 2 min. After that, the mold was opened and the sample was retrieved (thickness about 1.2 mm).

For MC, a Haake torque rheometer (Rheocord 500p) incorporating a mixer (Rheomix 600p) with twin-roller rotors was used for kneading the materials (Xue, Yu, Xie, Chen, & Li, 2008). The initial temperature was set to be 70 °C, the rotor speed was 70 rpm, and the mixing time was 8 min (Wang et al., 2010). After mixing, the samples were compression molded into films using the same method as described above for CM. Each sample in the mold was first hot-pressed in the upper area at a temperature of 120 °C and a pressure of 10 MPa for 2 min, which was then immediately moved to the lower area and pressed under 10 MPa for cooling for 2 min.

All the films were conditioned at 75% relative humidity (with oversaturated sodium chloride solution) for 7 days before any characterization of the materials. After the conditioning, the thickness of the films was 1.0–1.1 mm.

2.5 Characterization of starch-based films

2.5.1 Scanning electron microscopy (SEM)

The morphology of normal and fracture surfaces of starch-based films was examined using a scanning electron microscope (JEOL JSM-7001F, Tokyo, Japan) with an accelerating voltage of 3 kV and a spot size of 6 nm. Starch-based films were cryo-ground in liquid nitrogen to obtain fracture surfaces and the pieces were then fixed onto circular metal stubs previously covered with double-sided adhesive, followed by platinum coating for a 5-nm thickness using an Eiko sputter coater under vacuum.

2.5.2 X-ray diffraction (XRD)

X-ray diffraction (XRD) analysis was performed with an Xpert PRO diffractometer (PANalytical B.V., Netherlands) operated at 40 mA and 40 kV using Cu Kα radiation with a wavelength of 0.1542 nm as the X-ray source. The scanning was carried out with the diffraction angle (2θ) from 5° to 50° with a scanning speed of 10°/min and a scanning step of 0.033°. The degrees of crystallinity of the samples were quantitatively estimated according to a previous study (Liu et al., 2009b). Specifically, a smooth curve connected with the peak baseline was plotted on the diffraction using the software. The area above the smooth curve was regarded as the crystalline portion, while the lower area between the smooth curve and the linear baseline was taken as the amorphous portion. The upper diffraction peak area and the total diffraction area were integrated by MDI Jade 6 software. The ratio of upper area to total diffraction area was taken as the degree of crystallinity.

2.5.3 Mechanical properties

The mechanical properties of starch-based films were determined using an Instron Universal Testing Machine (5566) with a 500-N load cell. The films were cut into dumbbell-shaped strips, according to ASTM D882-10. The testing was performed with a constant deformation rate of 10 mm/min at room temperature due to their relatively brittle nature. The tensile strength (σ_t) and elongation at break (ε_b) were determined by the Instron software from at least 7 specimens for each of the samples (Li et al., 2011).

2.5.4 Thermogravimetric analysis (TGA)

The thermal decomposition of starch-based materials was determined by a thermogravimetric analysis (TGA) apparatus (TGA4000, PerkinElmer, USA) under nitrogen condition. A sample mass of about 5 mg was used for each run. The samples were heated from 50 °C to 700 °C with a constant heating ramp of 50 K/min. The weight loss results were also converted into derivative weight loss to measure thermal decomposition temperatures. The temperature calibrations were undertaken by the Curie temperatures of nickel and iron.

2.6 Data analysis

Data were analyzed using a one-way analysis of variance (ANOVA) and Duncan's test for a statistical significance $p \leq 0.05$ using SPSS Statistics software (version 19.0).

3 Results and Discussion

3.1 Study of conformations in starch-$ZnCl_2$ solutions

3.1.1 Rheological study of starch/zinc mixed solutions

The relationships between viscosity and shear rate for Gelose 80 starch/$ZnCl_2$ solutions and waxy starch/$ZnCl_2$ solutions were established in **Fig. 1a** and **b**. It can be seen that, for $ZnCl_2$ aqueous solutions (without starch), although the viscosity increased with a higher $ZnCl_2$ concentration, the

viscosity was not varied by shear rate, suggesting that all the salt solutions exhibited Newtonian behavior. All the starch/$ZnCl_2$ solutions showed a shear-thinning behavior and could be considered as pseudoplastic fluids, which were typical of macromolecules in solution. Moreover, waxy starch/$ZnCl_2$ solutions present higher viscosities than Gelose 80 starch/$ZnCl_2$ solutions, which could be ascribed to the much higher molecular mass of waxy starch.

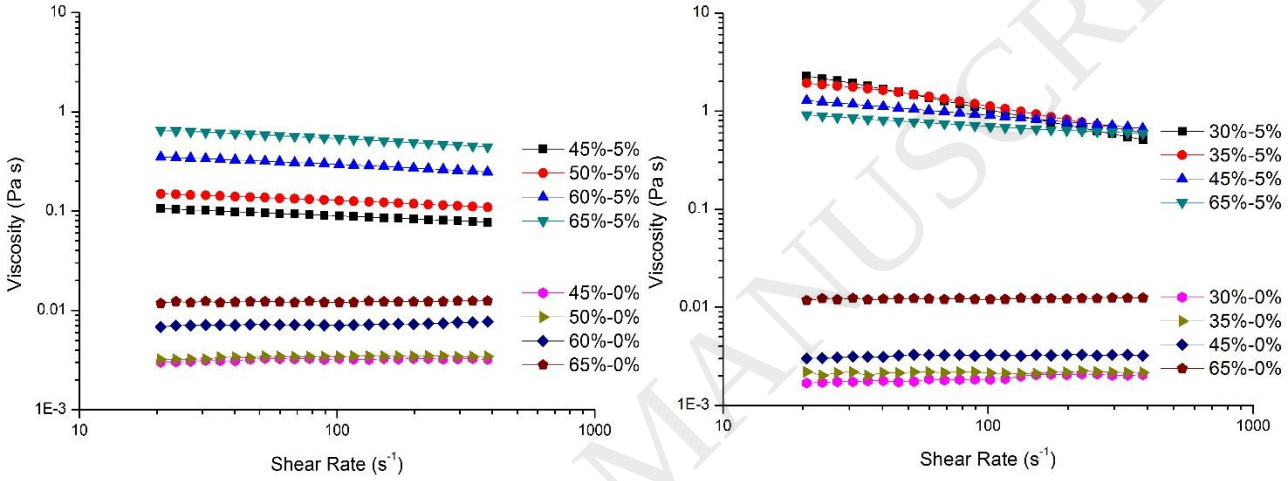

(a) (b)

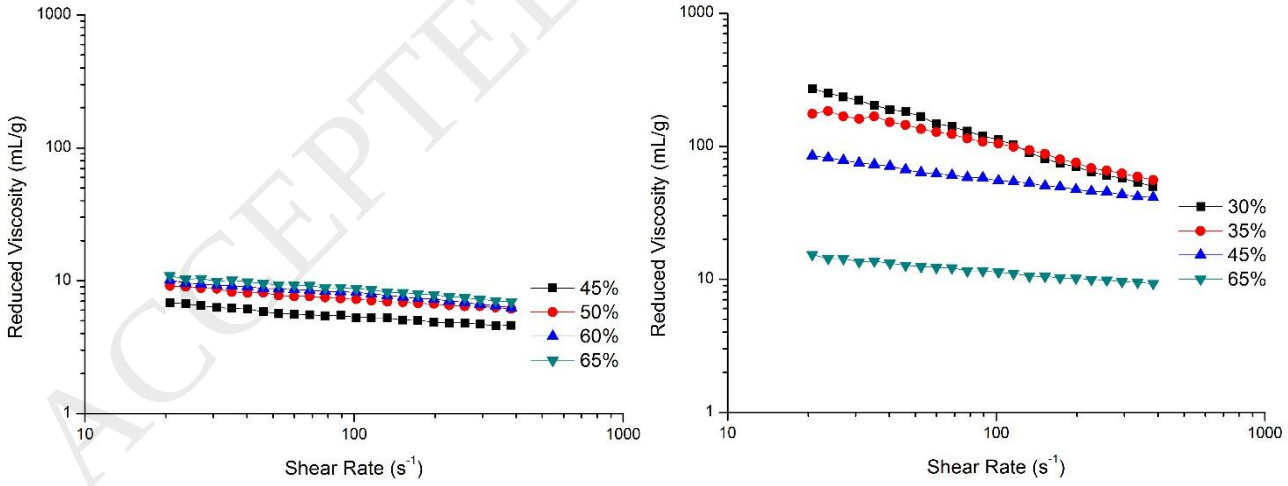

(c) (d)

Fig. 1.Viscosity vs. shear rate curves of Gelose 80 starch/$ZnCl_2$ solutions (a) and waxy starch/$ZnCl_2$ solutions (b); and reduced viscosity vs. shear rate curves of Gelose 80 starch/$ZnCl_2$ solutions (c)

and waxy starch/$ZnCl_2$ solutions (d). For all the results, the starch concentration was fixed at 5 wt.% and the temperature was set at 30 °C.

Concerning Gelose 80 starch (**Fig. 1a**), the viscosity vs. shear rate curves for different $ZnCl_2$ concentrations were parallel to each other and the viscosity of G80 starch/$ZnCl_2$ solutions increased with $ZnCl_2$ concentration. In contrast, for waxy starch (**Fig. 1b**), the viscosity vs. shear rate curves displayed varied slopes (and thus shear thinning behavior) with $ZnCl_2$ concentration. Increased $ZnCl_2$ concentrations could result in waxy starch/$ZnCl_2$ solutions with reduced shear-thinning behavior. It can also be seen that waxy starch/65% $ZnCl_2$ solution presents a slope similar to those of the different G80 starch/$ZnCl_2$ solutions of ≤65% $ZnCl_2$ concentrations. While previous studies have already demonstrated the complexation between Zn^{2+} ions and amylose (Luo et al., 2013; Luo et al., 2016), we propose that Zn^{2+} ions could also be complexed with amylopectin and this complexation is more apparent when the $ZnCl_2$ concentration is high (e.g., 45% and 65%). Based on these results, it is likely that the starch-zinc complexation could lead to reduced entanglement of macromolecules and thus a weakened shear-thinning effect.

According to the IUPAC (Mcnaught & Wilkinson, 2006), reduced viscosity is a classical viscosity parameter. It is the ratio of the relative viscosity increment versus the mass concentration of the solute polymers, and eliminates the influence of the solvent and reflects the changes of the solute conformation directly (Kulshreshtha, Singh, & Sharma, 1988; Nishida, Kaji, & Kanaya, 2001). The reduced viscosities of these solutions, which were calculated by **Eq.(1)** based on the data in **Fig. 1a** and **b**, were shown in **Fig. 1c** and **d,** respectively. For Gelose 80 (**Fig. 1c**), the reduced viscosity was

higher with a higher $ZnCl_2$ concentration, which could be due to the enlarged starch-zinc complexes. However, **Fig. 1d** shows a reverse trend for waxy starch, with a higher $ZnCl_2$ concentration leading to significantly lowered reduced viscosity. Compared with amylose, waxy starch has a much large molecular mass and contains many rigid, short branches. These may allow waxy starch molecules themselves to form a kind of gel-ball conformation (Xie et al., 2009), which can be reflected by reduced viscosity. When the $ZnCl_2$ concentration was high, the complexation between Zn^{2+} ion and amylopectin becomes more apparent and could weaken the original amylopectin conformation. Moreover, the possible acid hydrolysis of starch at high $ZnCl_2$ concentrations (Lin et al., 2016) might also contribute to the variation in reduced viscosity.

Besides the results in **Fig. 1**, we also studied the viscosity vs. shear rate for the same starch/$ZnCl_2$ solutions at 60 °C, and all of the rheological curves were not apparently varied by the temperature (**Fig. S1** in **Supplementary Data**).

3.1.2 Size distribution

While previous studies (Luo et al., 2013; Luo et al., 2016) have proposed an "amylose–zinc inclusion complex" conformation, the size of the complex has not been studied. In this work, the size distributions of particles in $ZnCl_2$ solutions were shown in **Fig. 2**. It can be seen that for both waxy and G80 starches, higher $ZnCl_2$ concentrations led to larger particle sizes. As in this case, starch should be completely dissolved in $ZnCl_2$ solution (Lin et al., 2016), the formation of particles could only be due to the complexation between starch and Zn^{2+} ion. Our results show that this complexation could be effectively facilitated by a higher $ZnCl_2$ concentration. As the complexation is

irrespective of the starch type (waxy or high-amylose starch), both amylose and amylopectin could interact with Zn^{2+} ions to form complexes, which corresponds to the rheological results as discussed before. Nevertheless, the interaction between starch and Zn^{2+} ion is worth further investigation.

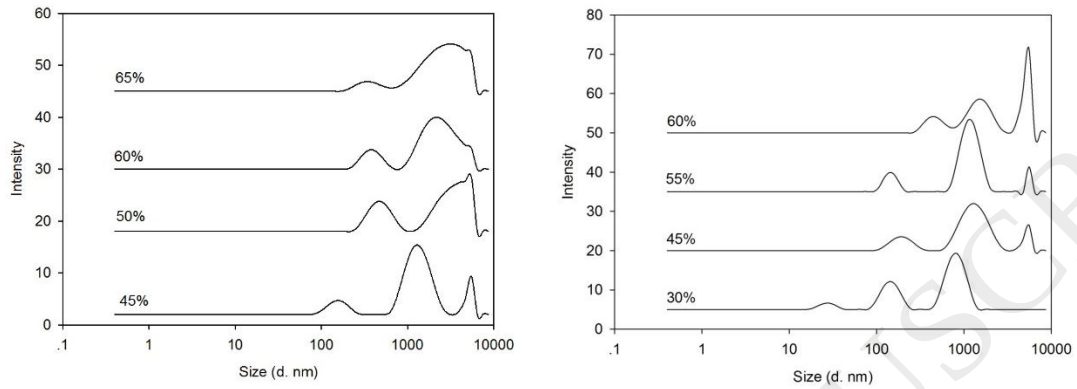

(a) (b)

Fig. 2.Size distributions of Gelose 80 (a) and waxy (b) starch particles in $ZnCl_2$ solutions. The concentration of starch was fixed at 1%.

3.2 Reinforcement effect of the starch-zinc complexes on starch-based films

3.2.1 Morphology of starch-based films

Fig. 3a–d show the normal and fracture surfaces of G-15/CM and W-15/CM. It can be seen that starch granules had been melted to form materials. The normal surfaces (**Fig. 4a** and **c**) were uneven with some remaining granules or granule residues. Nonetheless, the sections of the samples (**Fig. 4b** and **d**) seemed to be smooth and homogeneous with starch granule remnants much less apparent. Therefore, 15% $ZnCl_2$ solution could be considered to be effective for the phase transition and plasticization of starch (even Gelose 80 high-amylose starch) by CM at 120 °C. All the starch-based

films are transparent, suggesting excellent plasticization. Since CM involves little shear treatment (Xie et al., 2014; Zhang et al., 2017) and the temperature here (120 °C) was lower than that (160 °C) used in a previous study for the preparation of Gelose 80 starch-based materials plasticized by water–glycerol or water–ionic liquid mixtures (Xie et al., 2015; Zhang et al., 2016), the excellent plasticization effect of $ZnCl_2$ solutions is demonstrated.

Fig. 3e–h show the normal and fracture surfaces of G-25/MC and W-30/MC. As expected, shear force could facilitate the melting of starch granules. Unlike the CM samples, the MC samples showed minimal granule remnants.

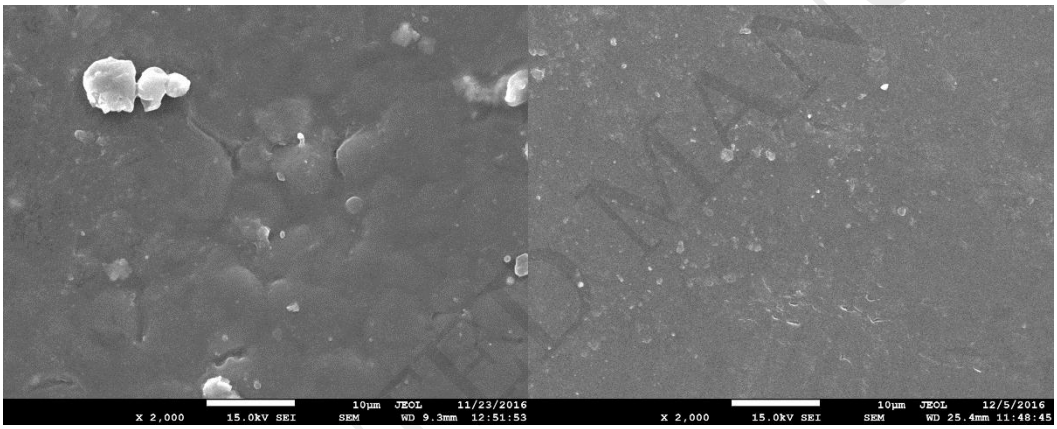

(a) (b)

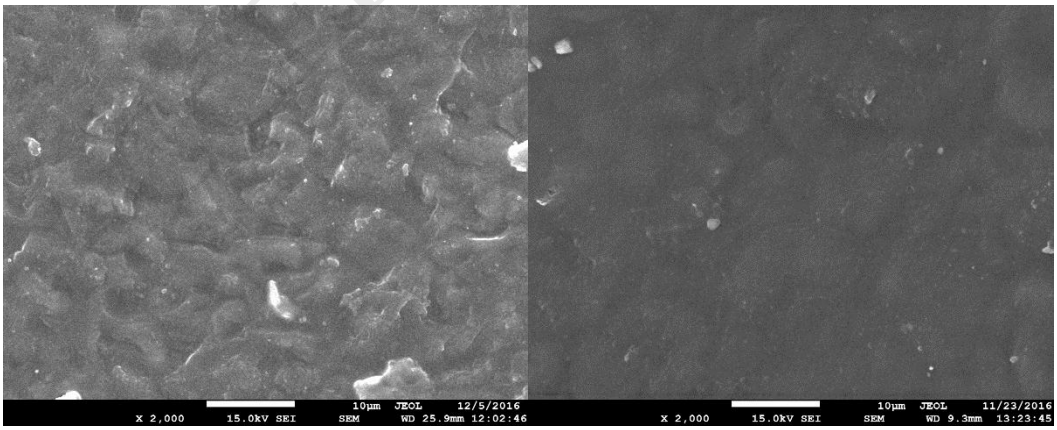

(c) (d)

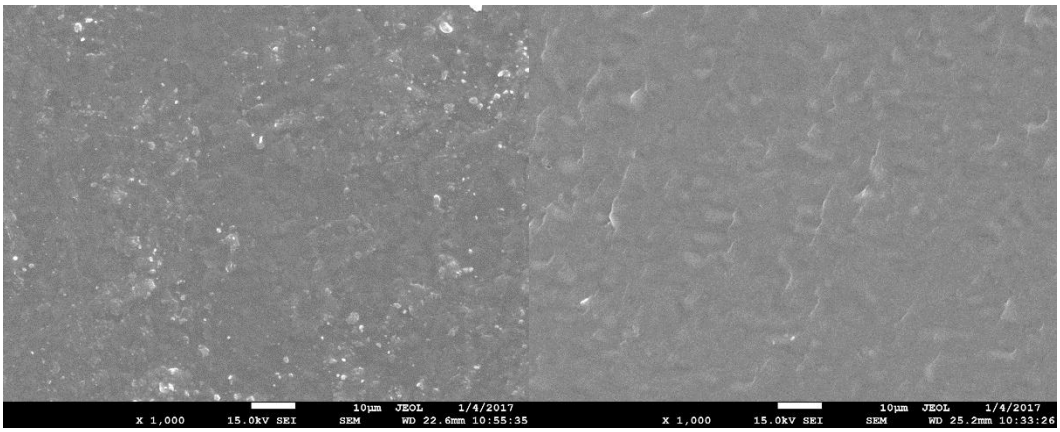

(e) (f)

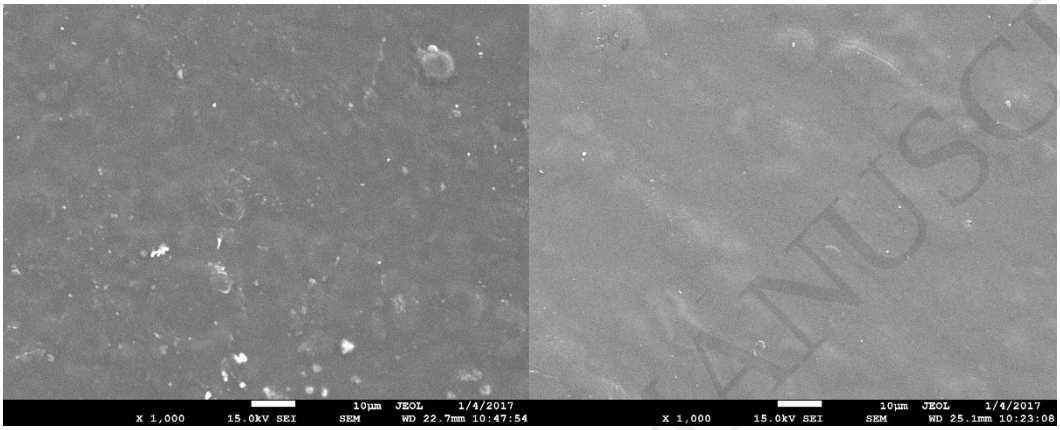

(g) (h)

Fig. 3. SEM images of starch-based films. (a) and (b) were the normal surface and the fracture surface of G-15/CM, (c) and (d) were those of W-15/CM, (e) and (f) were those of G-25/MC, and (g) and (h) were those of W-30/MC, respectively.

3.2.2 XRD results of starch-based films

Fig. 4a shows that for G-0/CM (G80 starch-based films prepared with only water), the crystalline peaks located at 13°, 15°, 17°, 19.5°, 22° and 24°, which indicate the B-type crystalline structure of starch (Lopez-Rubio, Flanagan, Gilbert, & Gidley, 2008). For G80 starch-based films plasticized by $ZnCl_2$ solutions, except the 19.5° crystalline peak, the intensities of other peaks were

gradually reduced with higher $ZnCl_2$ concentrations. When the $ZnCl_2$ concentration was higher than 20%, the peaks at 13° and 15° almost vanished. Nonetheless, the 19.5° crystalline peak became sharper when the $ZnCl_2$ concentration was lower than 25% while turned out to be weaker with higher $ZnCl_2$ concentrations. Since this peak was characteristic of the single-helical amylose structure (Lopez-Rubio et al., 2008), it could demonstrate the formation of starch–zinc inclusion complexes. As this starch-zinc complexes might exist in the regenerated starch, Fourier-transform infrared (FTIR) (**Fig. S2**, **Supplementary Data**) and ^{13}C nuclear magnetic resonance (NMR) (**Fig. S3**, **Supplementary Data**) techniques were used to investigate the different between native and regenerated starches. No significant difference could be observed from FTIR results. NMR spectra indicate apparent shifts of the C-1, C-4 and C-6 absorption peaks to lower field, which could be due to the starch-zinc interactions and to the formation of amylose inclusion complexes (Luo et al., 2013; Luo et al., 2016).

For G80 starch-based films (**Fig. 4c**), although the intensity of all crystalline peaks was reduced with higher $ZnCl_2$ concentrations, the peaks (13°, 15°, 17°, 19.5°, 22° and 24°) could still be observed even prepared with 40% $ZnCl_2$ solution, and no peak became sharp or vanished, which is different from the results in **Fig. 4a**. As all these are the XRD data of the conditioned samples and recrystallization could occur during conditioning, it is proposed that the MC samples had a higher tendency to recrystallize to form new B-type crystals and a single-helical amylose structure. Along with the morphological observation, it was likely that an additional mixing process could facilitate the plasticization of starch-based materials and promote the interactions between starch chains, which was instrumental to the subsequent recrystallization.

On the other hand, for waxy starch-based films (**Fig. 4b** and **d**), no matter they were plasticized by water or by $ZnCl_2$ solution, or prepared by CM or by MC, their crystalline peaks always located at 15°, 17°, 18° and 23°, which are characteristic of the A-type crystalline structure. The higher $ZnCl_2$ concentration only led to the reduced intensity of these peaks. Regarding this, we consider that as waxy starch is much easier to be plasticized than a higher-amylose starch (Li et al., 2011; Liu et al., 2006; Liu et al., 2011; Wang et al., 2010), the effect of the additional mixing on recrystallization became insignificant.

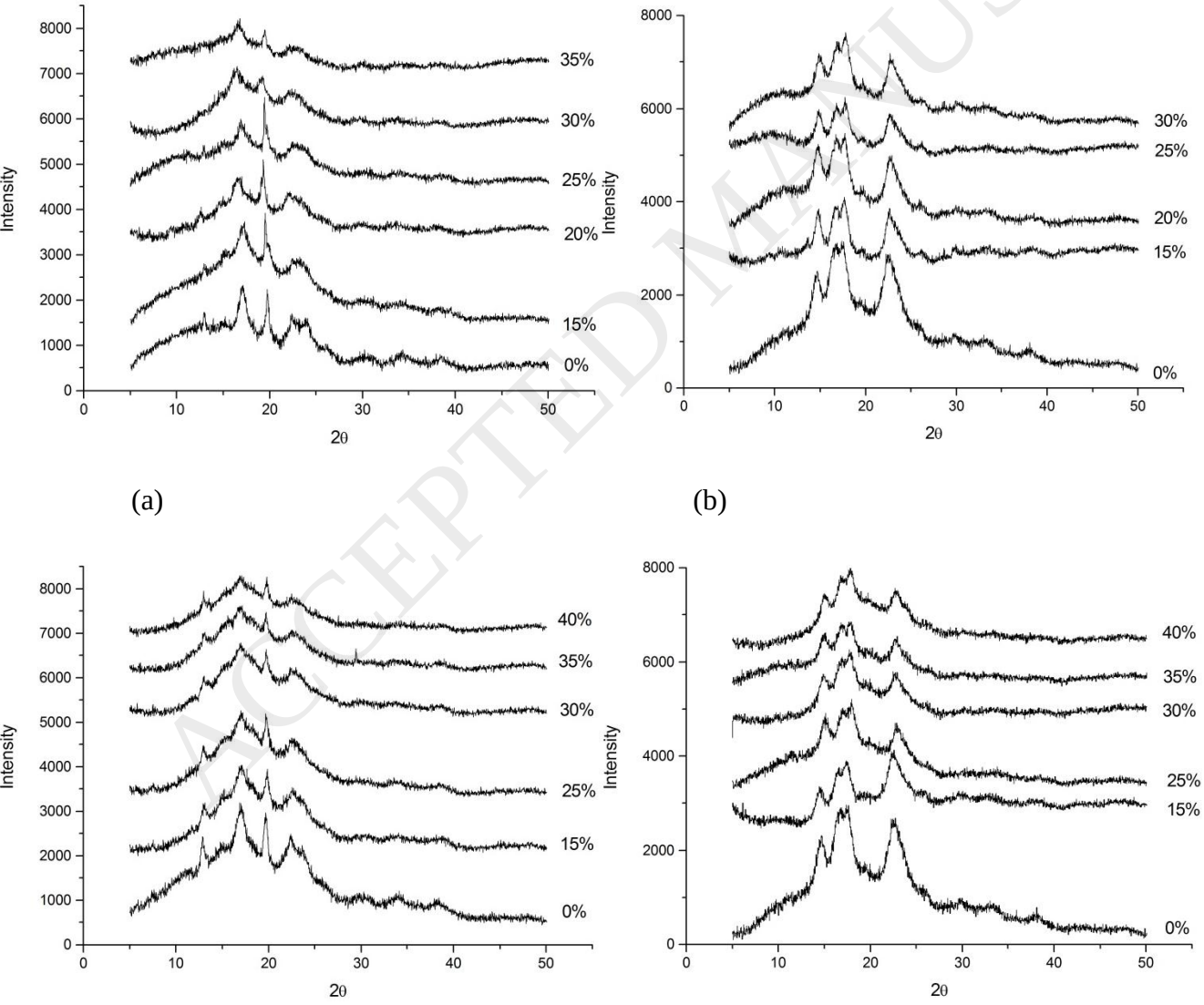

(c) (d)

Fig. 4. XRD patterns of G80 (a) and waxy (b) starch-based films prepared by CM; and of G80 (c) and waxy (d) starch-based films prepared by MC.

Calculated from the XRD curves in **Fig. 4**, **Table 1** lists the crystallinity data of the samples. It can be seen that for all the samples, the degree of crystallinity was decreased with the increased $ZnCl_2$ concentration. Regarding this, $ZnCl_2$ solutions could present a stronger plasticization effect, especially at higher concentrations. The degrees of crystallinity of the samples here were lower than those of Gelose 80 starch-based films plasticized by water–glycerol or water–ionic liquid mixtures (Xie et al., 2014). This, again, demonstrates the excellent plasticization effect of $ZnCl_2$ solutions. Besides, just like water–ionic liquid mixtures, $ZnCl_2$ solutions could effectively prevent the post-processing recrystallization of starch-based materials. Moreover, **Table 1** shows that, again, G80 starch-based materials prepared by MC had slightly higher degrees of crystallinity than those prepared by CM under the same formulations, which could be due to the positive effect of mixing on the interactions between starch chains and the subsequent recrystallization.

3.2.3 Mechanical properties of starch-based films

Fig. 5a and **b** show the mechanical properties of G80 and waxy starch-based films prepared by CM. Firstly, the mechanical properties were less affected by the starch type but more by the $ZnCl_2$ concentration. The mechanical strength values of G80 starch-based films plasticized by $ZnCl_2$ solutions are similar to those of similar films plasticized by the water–glycerol mixtures and water–

ionic liquid mixtures in the earlier study (Xie et al., 2014). For all the materials, both their tensile strength and elongation at break initially increased with increasing $ZnCl_2$ concentration. After reaching a peak, both of them descended with a further increase in $ZnCl_2$ concentration. More specifically, for G80 starch-based films, the greatest tensile strength (29.3±2.7 MPa) appeared at 25% $ZnCl_2$ concentration while 20% $ZnCl_2$ concentration led to the highest elongation at break (20.2±3.9 %). For waxy starch-based films, both the highest tensile strength (29.0±2.3 MPa) and the highest elongation at break (14.6±2.5 %) occurred at 20% $ZnCl_2$ concentration. These results could be contributed by different factors such as the plasticization of starch by $ZnCl_2$ solution (the interaction between starch chains and $ZnCl_2$), the interactions between starch chains (which could lead to recrystallization), and the reinforcement by starch-zinc complexes. It is noteworthy that the crystallinity as shown by XRD data could be contributed by both original native starch crystals as well as the recrystallized structure. We consider 20% or 25% $ZnCl_2$ concentration could be optimal for achieving the necessary starch chain interactions and the best reinforcement effect by starch-zinc complexes, which were responsible for both the increased tensile strength and elongation at break. When the $ZnCl_2$ concentration was too high, the starch interchain forces could be reduced and the formation of new crystals and starch-zinc complexes became difficult. Besides, the acidity of solutions might cause the hydrolysis of starch macromolecular chains (Lin et al., 2016). All of these factors could result in weakened mechanical properties.

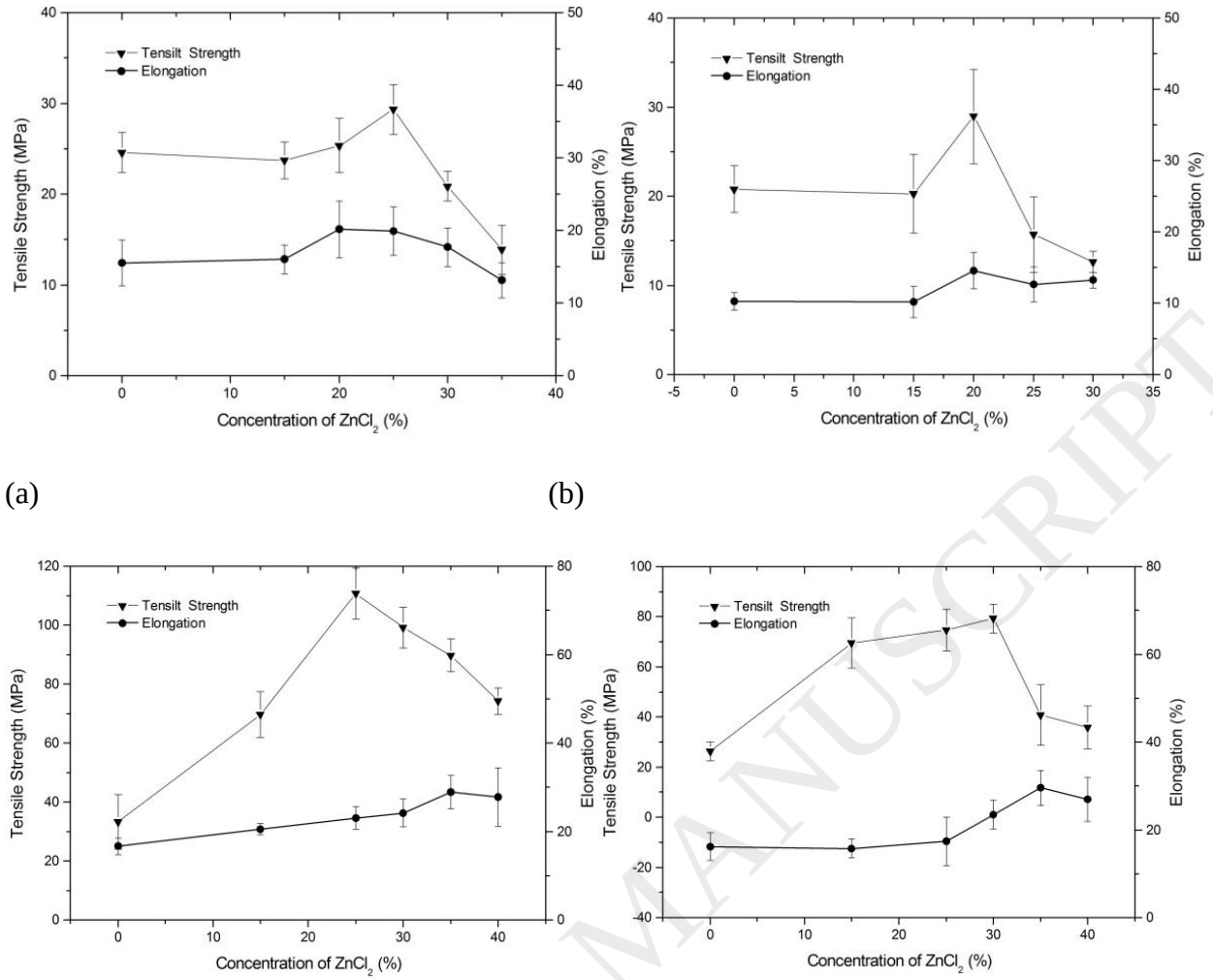

Fig. 5. Mechanical properties of G80 (a) and waxy (b) starch-based films prepared by CM; and of G80 (c) and waxy (d) starch-based films prepared by MC.

Fig. 5c and **d** show the mechanical properties of starch-based films prepared by MC. Similar to the case of CM, both the tensile strength and the elongation at break first increased to reach a peak and then decreased irrespective of the starch type. More specifically, for G80 starch-based films, the greatest tensile strength (110.7±8.6 MPa) appeared at 25% $ZnCl_2$ concentration while 35% $ZnCl_2$ concentration led to the highest elongation at break (29.0±3.8%). For waxy starch-based films, the

greatest tensile strength (79.3±5.7 MPa) occurred at 30% $ZnCl_2$ concentration while the maximal elongation at break (29.6±4.0%) appeared at 35% $ZnCl_2$ concentration. Again, the greatly enhanced mechanical properties could be contributed by the reinforcement by starch-zinc complexes as well as molecular interactions and recrystallization. Interestingly, with the same formulation, MC could give higher tensile strength values, which are more than three times those of the CM samples. The tensile strength data obtained here are even higher than those of starch-based materials plasticized by water, water–glycerol, or water–ionic liquid mixtures (Xie et al., 2014). More importantly, the dramatic increase in tensile strength was not at the cost of the elongation at break. The elongation at break was even moderately increased by changing from CM to MC. Given this, it is proposed that the mixing process could dramatically disrupt the original starch structure and promote the interactions between starch chains and between starch chains and starch-zinc complexes, and thus enhancing the reinforcement effect of starch-zinc complexes. Considering that waxy starch-based films prepared by MC did not show higher crystallinity than those prepared by CM, such intermolecular interactions could have played a major role in enhancing the mechanical properties.

3.2.4 TGA

Thermogravimetric analysis (TGA) was used to understand the thermal stability of starch-based films as influenced by $ZnCl_2$ solution (**Fig. 6**). Without $ZnCl_2$, Gelose 80 starch-based films experienced thermal decomposition between 300 °C and 350 °C. Irrespective of the preparing method, this thermal decomposition temperature of starch was dramatically reduced to be below 300 °C with the addition of $ZnCl_2$ solution. A previous study (Xie et al., 2014) has shown that ionic

liquid-plasticized starch-based materials also displayed a significantly reduced thermal decomposition temperature. Due to the early degradation of starch, the content of $ZnCl_2$ involved in the formation of starch-zinc complexes is unknown from TGA. This is worthy further investigation.

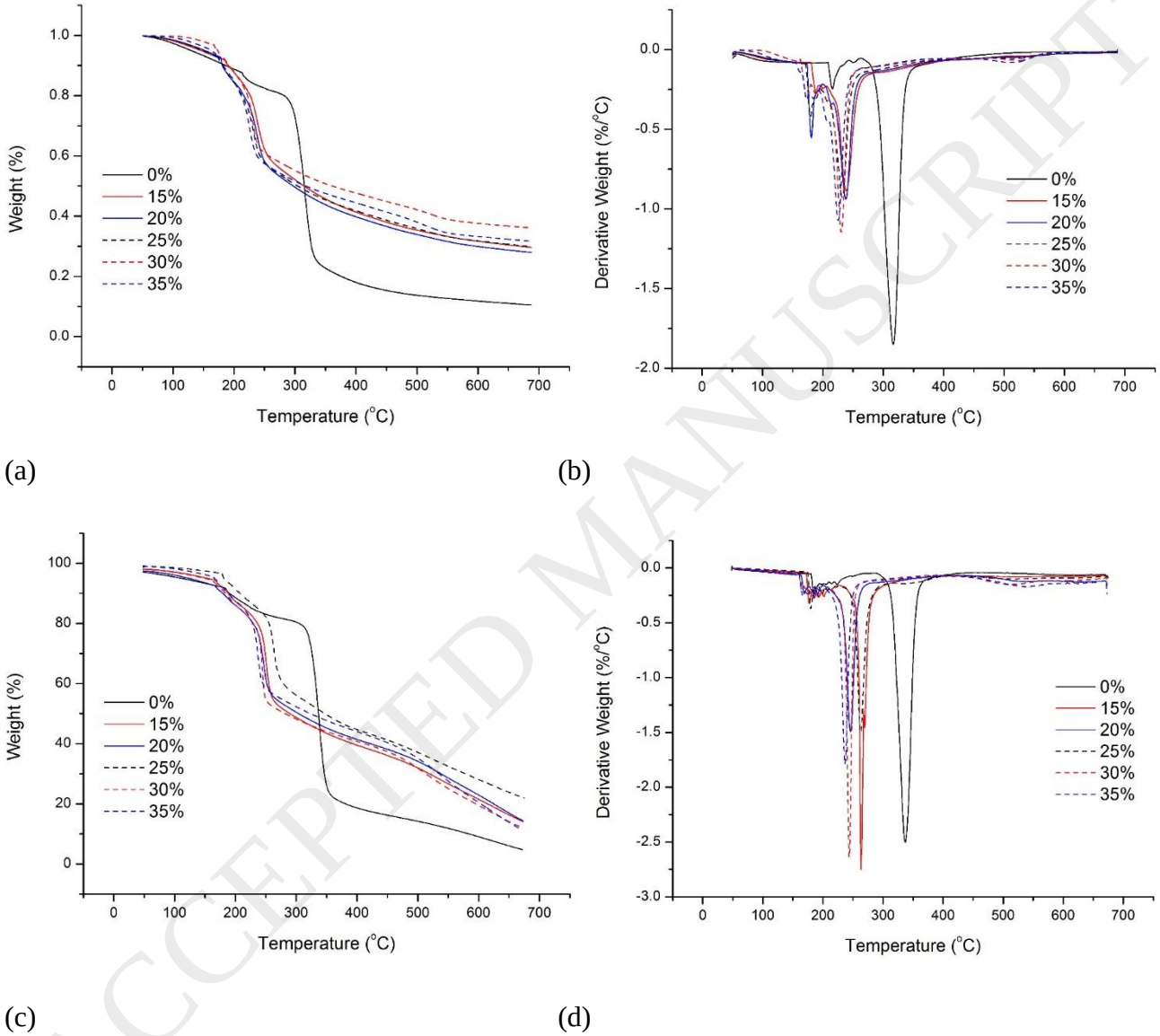

Fig. 6. Weight loss and derivative weight loss of Gelose 80 starch-based materials prepared by CM (a and b) and by MC (c and d) with $ZnCl_2$ solutions of different concentrations.

3.3 Discussion

Previous studies (Luo et al., 2013; Luo et al., 2016; Sahin & Sumnu, 2006) have proposed the amylose–zinc inclusion complexes and verified the covalent bonds between Zn^{2+} ions and starch chains by Raman spectroscopy. Specifically, a Zn^{2+} cation is mainly coordinated to the oxygen atoms of the glucose unit 6-CH_2OH, and inserts into the helices of starch chains to form the amylose–zinc inclusion complexes, just like the conformation of a metal chelator. On the other hand, since Cl^- anions only have the protonation effect in the presence of moisture to catalyze the depolymerization of starch (Kärkkäinen, Lappalainen, Joensuu, & Lajunen, 2011; Stevenson, Biswas, Jane, & Inglett, 2007; Zhang et al., 2015). However, these aspects are not enough to account for the enhanced mechanical properties.

The "cellulose–zinc complex" conformation has also been proposed (Jian, Ye, & Zhao, 2010; Wei & Wu, 2017). Specifically, since a Zn^{2+} cation has two positive charges, it can accept two pairs of isolated charges on the oxygen atoms of hydroxyls on cellulose. In other words, each Zn^{2+} ion can interact with two glucopyranoses of cellulose. Regarding the experimental results and the previously proposed conformation, although starch helical chains are different from the straight chains of cellulose, there are plenty of 6-CH_2OH on starch chains. It is considered here that a Zn^{2+} cation can either interact with two 6-CH_2OH groups from one starch chain to form an amylose–zinc inclusion complex, or with two 6-CH_2OH groups from two starch chains to link neighboring starch molecular chains, as illustrated in **Fig. 7**. The similar complex has been mentioned by other researchers (Ciesielski & Tomasik, 2004; Lai, Tomasik, Yen, Hung, & Lii, 2002; Szymońska, Molenda, & Wieczorek, 2015). Because of the intermolecular binding of St-O-Zn-O-St bridges, the starch-zinc

complex can enlarge with the rise in $ZnCl_2$ concentration. The starch-zinc complex could act as a reinforcing agent to increase the mechanical properties of starch-based materials.

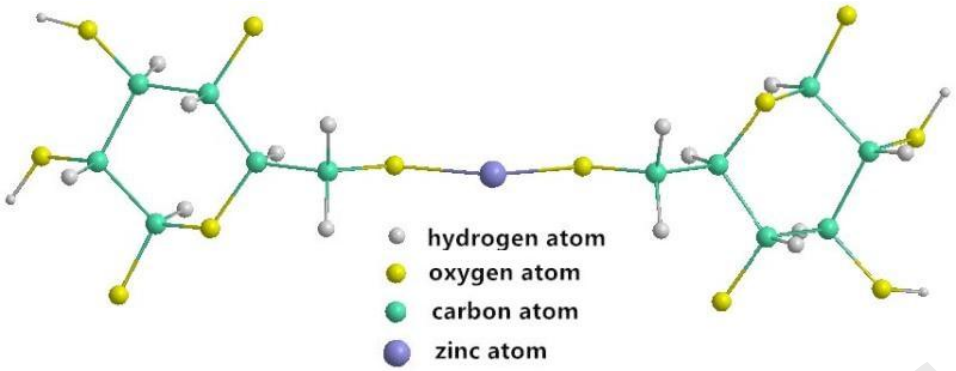

(a)

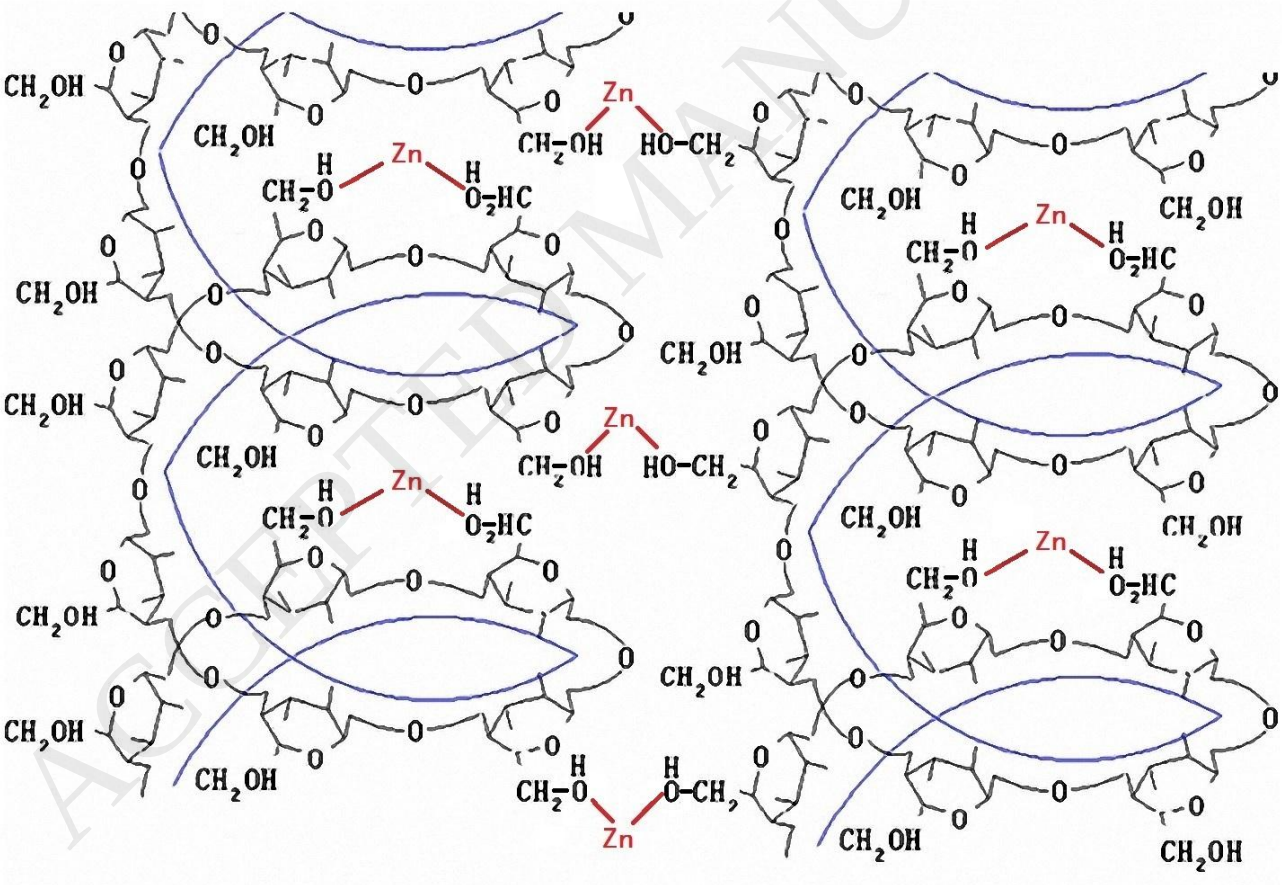

(b)

Fig. 7.Schematic of starch-zinc complex conformation.

4 Conclusions

Under solution conditions, starch-zinc complexes were found to be enlarged with the increased $ZnCl_2$ concentration. It is considered that a Zn^{2+} ion can either interact with two 6-CH_2OH group from one starch chain to form an "amylose–zinc inclusion complex", or with two 6-CH_2OH group from two starch chains to link neighboring starch molecular chains.

By CM, well-plasticized starch-based films could be obtained at 120 °C with 15 wt.% $ZnCl_2$ solution, which demonstrated its excellent plasticization effect. Both the tensile strength and elongation at break of materials increased with a rise in $ZnCl_2$ concentration, which could be mainly contributed by the reinforcement by starch-zinc complexes and the enhanced molecular interactions. By changing the processing protocol from CM to MC, the tensile strength of starch-based films could be significantly increased (more than three times). It is proposed that the shear treatment in MC facilitated the molecular interactions within the materials, which supplemented the reinforcement effect of starch-zinc complexes. Irrespective of the processing method, the addition of $ZnCl_2$ solutions could significantly reduce the thermal stability of starch-based materials.

Our results here have demonstrated that $ZnCl_2$ solutions can play both as a plasticization and reinforcement agent for starch-based materials. As there are many similar salt ions with activated electronic orbits, which can accept isolated charges pairs on the oxygen atoms of hydroxyls on starch, more research is desired focusing on a wide range of metal ions.

Acknowledgements

The research leading to these results has received funding from the National Natural Science Foundation of China (NSFC) (Project No. 21106023), the "Pearl River S&T Novel Program of Guangzhou" (Project No. 201610010019), and the National Natural Science Foundation of Guangdong Province (No. 2018A0303130048). Besides, the authors also thank for the financial support provided by "The Foundation for Fostering the Scientific and Technical Innovation of Guangzhou University". F. Xie acknowledges the European Union's Marie Skłodowska-Curie Actions (MSCA) and the Institute of Advanced Study (IAS), University of Warwick for the Warwick Interdisciplinary Research Leadership Programme (WIRL-COFUND).

The authors have declared no conflict of interest.

References

Ali, A., Xie, F., Yu, L., Liu, H., Meng, L., Khalid, S., et al. (2018). Preparation and characterization of starch-based composite films reinfoced by polysaccharide-based crystals. *Composites Part B: Engineering, 133*, 122-128.

Bahruddin, Hendri, Z. O., Rifaldi, A., Syaputra, A. F., & Rochaeni, U. A. (2018). Properties of Sago Starch-Based Biopolymers with Clay, Cellulose, Zinc Oxide and Chitosan Fillers. *Materials Science Forum, 917*, 32-36.

Bie, P., Liu, P., Yu, L., Li, X., Chen, L., & Xie, F. (2013). The properties of antimicrobial films derived from poly(lactic acid)/starch/chitosan blended matrix. *Carbohydrate Polymers, 98*(1), 959-966.

Cao, L., Long, Y., Pei, C., Ling, C., Wei, Z., George, S., et al. (2010). Design, Preparation and Characterization of Self‐Reinforced Starch Films through Chemical Modification. *Macromolecular Materials and Engineering, 295*(11), 1025-1030.

Chen, T.-S., & Joslyn, M. A. (1967). The effect of sugars on viscosity of pectin solutions: II. Comparison of dextrose, maltose, and dextrins. *Journal of Colloid and Interface Science, 25*(3), 346-352.

Chen, X., Liu, P., Shang, X., Xie, F., Jiang, H., & Wang, J. (2017). Investigation of rheological properties and conformation of cassava starch in zinc chloride solution. *Starch - Stärke, 69*(9-10), 1600384-n/a.

Ciesielski, W., Lii, C.-y., Yen, M.-T., & Tomasik, P. (2003). Interactions of starch with salts of metals from the transition groups. *Carbohydrate Polymers, 51*(1), 47-56.

Ciesielski, W., & Tomasik, P. (2004). Complexes of amylose and amylopectins with multivalent metal salts. *Journal of Inorganic Biochemistry, 98*(12), 2039-2051.

Correa, A. C., Carmona, V. B., Simão, J. A., Capparelli Mattoso, L. H., & Marconcini, J. M. (2017). Biodegradable blends of urea plasticized thermoplastic starch (UTPS) and poly(ε-caprolactone) (PCL): Morphological, rheological, thermal and mechanical properties. *Carbohydrate Polymers, 167*, 177-184.

Fazeli, M., Keley, M., & Biazar, E. (2018). Preparation and characterization of starch-based composite films reinforced by cellulose nanofibers. *International Journal of Biological Macromolecules, 116*, 272-280.

Fischer, S., Leipner, H., Thümmler, K., Brendler, E., & Peters, J. (2003). Inorganic Molten Salts as Solvents for Cellulose. *Cellulose, 10*(3), 227-236.

Iamareerat, B., Singh, M., Sadiq, M. B., & Anal, A. K. (2018). Reinforced cassava starch based edible film incorporated with essential oil and sodium bentonite nanoclay as food packaging material. *Journal of Food Science and Technology, 55*(5), 1953-1959.

Ibrahim, H., Mehanny, S., Darwish, L., & Farag, M. (2018). A Comparative Study on the Mechanical and Biodegradation Characteristics of Starch-Based Composites Reinforced with Different Lignocellulosic Fibers. *Journal of Polymers and the Environment, 26*(6), 2434-2447.

Jian, X., Ye, J., & Zhao, X. F. (2010). Solubility of Cellulose in ZnCl_2 Aqueous Solution and Structure of Regenerated Cellulose. *Journal of South China University of Technology (Natural Science Edition), 38*(2), 23-27.

Kang, Z., XiaoPing, C., Fei, C., Yi, L., Mi, Z., & PuXin, Z. (2018). Poly(citrate glyceride): a hyperbranched polyester for starch plasticization. *Polymer International, 67*(4), 399-404.

Kärkkäinen, J., Lappalainen, K., Joensuu, P., & Lajunen, M. (2011). HPLC-ELSD analysis of six starch species heat-dispersed in [BMIM]Cl ionic liquid. *Carbohydrate Polymers, 84*(1), 509-516.

Kulshreshtha, A. K., Singh, B. P., & Sharma, Y. N. (1988). Viscometric determination of compatibility in PVC/ABS polyblends—II. Reduced viscosity-concentration plots. *European Polymer Journal, 24*(1), 33-35.

Kweon, D. K., Choi, J. K., Kim, E. K., & Lim, S. T. (2001). Adsorption of divalent metal ions by succinylated and oxidized corn starches. *Carbohydrate Polymers, 46*(2), 171-177.

Lai, V. M. F., Tomasik, P., Yen, M.-T., Hung, W.-L., & Lii, C.-y. (2002). Re-examination of the interactions between starch and salts of metals from the non-transition groups. *International Journal of Food Science & Technology, 36*(3), 321-330.

Leipner, H., Fischer, S., Brendler, E., & Voigt, W. (2000). Structural changes of cellulose dissolved in molten salt hydrates. *Macromolecular Chemistry & Physics, 201*(15), 2041-2049.

Li, M., Liu, P., Zou, W., Yu, L., Xie, F., Pu, H., et al. (2011). Extrusion processing and characterization of edible starch films with different amylose contents. *Journal of Food Engineering, 106*(1), 95-101.

Lin, M., Shang, X., Liu, P., Xie, F., Chen, X., Sun, Y., et al. (2016). Zinc chloride aqueous solution as a solvent for starch. *Carbohydrate Polymers, 136*, 266-273.

Liu, B., & Jin, N. (2016). The Applications of Ionic Liquid as Functional Material: A Review. *Current Organic Chemistry, 20*(20), 2109-2116.

Liu, H., Yu, L., Xie, F., & Chen, L. (2006). Gelatinization of cornstarch with different amylose/amylopectin content. *Carbohydrate Polymers, 65*(3), 357-363.

Liu, H., Xie, F., Yu, L., Chen, L., & Li, L. (2009a). Thermal processing of starch-based polymers. *Progress in Polymer Science, 34*(12), 1348-1368.

Liu, H., Yu, L., Simon, G., Zhang, X., Dean, K., & Chen, L. (2009b). Effect of annealing and pressure on microstructure of cornstarches with different amylose/amylopectin ratios. *Carbohydrate Research, 344*(3), 350-354.

Liu, P., Xie, F., Li, M., Liu, X., Yu, L., Halley, P. J., et al. (2011). Phase transitions of maize starches with different amylose contents in glycerol-water systems. *Carbohydrate Polymers, 85*(1), 180-187.

Liu, W., & Budtova, T. (2013). Dissolution of unmodified waxy starch in ionic liquid and solution rheological properties. *Carbohydrate Polymers, 93*(1), 199-206.

Lopez-Rubio, A., Flanagan, B. M., Gilbert, E. P., & Gidley, M. J. (2008). A novel approach for calculating starch crystallinity and its correlation with double helix content: A combined XRD and NMR study. *Biopolymers, 89*(9), 761-768.

Lu, X., & Shen, X. (2011). Solubility of bacteria cellulose in zinc chloride aqueous solutions. *Carbohydrate Polymers, 86*(1), 239-244.

Luo, Z., Cheng, W., Chen, H., Fu, X., Peng, X., Luo, F., et al. (2013). Preparation and Properties of Enzyme-Modified Cassava Starch–Zinc Complexes. *Journal of agricultural and food chemistry, 61*(19), 4631-4638.

Luo, Z., Zou, J., Chen, H., Cheng, W., Fu, X., & Xiao, Z. (2016). Synthesis and characterization of amylose–zinc inclusion complexes. *Carbohydrate Polymers, 137*, 314-320.

Ma, J., Zhu, W., Tian, Y., & Wang, Z. (2016). Preparation of Zinc Oxide-Starch Nanocomposite and Its Application on Coating. *Nanoscale Research Letters, 11*(1), 200.

Magdalena, Z., & Caisa, J. (2017). Impact of additives on mechanical and barrier properties of starch‐based films plasticized with deep eutectic solvents. *Starch - Stärke, 69*(11-12), 1700030.

Mcnaught, A. D., & Wilkinson, A. (2006). *IUPAC Compendium of Chemical Terminology*.

Nadanathangam, V., Sampath, K., Kathe, A. A., Varadarajan, P. V., & Virendra, P. (2006). Functional finishing of cotton fabrics using zinc oxide–soluble starch nanocomposites. *Nanotechnology, 17*(20), 5087.

Nagy, E. M., Coţa, C., Cioica, N., Gyorgy, Z., Todica, M., & Cozar, O. (2017). FT-IR investigation of starch based composite reinforced with Miscanthus fibers. *AIP Conference Proceedings, 1917*(1), 040009.

Nishida, K., Kaji, K., & Kanaya, T. (2001). Theoretical calculation of reduced viscosity of polyelectrolyte solutions. *Polymer, 42*(21), 8657-8662.

Para, A. (2004). Complexation of metal ions with dioxime of dialdehyde starch. *Carbohydrate Polymers, 57*(3), 277-283.

Para, A., Karolczyk-Kostuch, S., & Fiedorowicz, M. (2004). Dihydrazone of dialdehyde starch and its metal complexes. *Carbohydrate Polymers, 56*(2), 187-193.

Rychter, P., Kot, M., Bajer, K., Rogacz, D., Šišková, A., & Kapuśniak, J. (2016). Utilization of starch films plasticized with urea as fertilizer for improvement of plant growth. *Carbohydrate Polymers, 137*, 127-138.

Sahin, S., & Sumnu, S. G. (2006). Rheological Properties of Foods. *Physical Properties of Foods* (pp. 39-105). New York, NY: Springer New York.

Sheikhi, A., & van de Ven, T. G. M. (2018). Colloidal Starch and Cellulose Nanocrystals Unite To Improve the Mechanical Properties of Paper: From Enhanced Coatings to Reinforced Nanocomposites. *ACS Applied Nano Materials, 1*(4), 1841-1852.

Stevenson, D. G., Biswas, A., Jane, J.-l., & Inglett, G. E. (2007). Changes in structure and properties of starch of four botanical sources dispersed in the ionic liquid, 1-butyl-3-methylimidazolium chloride. *Carbohydrate Polymers, 67*(1), 21-31.

Szymońska, J., Molenda, M., & Wieczorek, J. (2015). Study of quantitative interactions of potato and corn starch granules with ions in diluted solutions of heavy metal salts. *Carbohydrate Polymers, 134*, 102-109.

Tajuddin, S., Xie, F., Nicholson, T. M., Liu, P., & Halley, P. J. (2011). Rheological properties of thermoplastic starch studied by multipass rheometer. *Carbohydrate Polymers, 83*(2), 914-919.

Tang, Y., Xie, F., Zhang, D., Zhu, M., Liu, L., Liu, P., et al. (2015). Physical properties and prebiotic activity of maize starch-based functional films. *Starch - Stärke, 67*(1-2), 124-131.

Thuy Pham, T. P., Cho, C.-W., & Yun, Y.-S. (2010). Environmental fate and toxicity of ionic liquids: A review. *Water Research, 44*(2), 352-372.

Wang, H., Gurau, G., & Rogers, R. D. (2012). Ionic liquid processing of cellulose. *Chemical Society Reviews, 41*(4), 1519-1537.

Wang, J., Yu, L., Xie, F., Chen, L., Li, X., & Liu, H. (2010). Rheological properties and phase transition of cornstarches with different amylose/amylopectin ratios under shear stress. *Starch/Stärke, 62*(12), 667-675.

Wei, W., & Wu, S. (2017). Depolymerization of cellulose into high-value chemicals by using synergy of zinc chloride hydrate and sulfate ion promoted titania catalyst. *Bioresource Technology, 241*, 760-766.

Wilpiszewska, K., & Spychaj, T. (2011). Ionic liquids: Media for starch dissolution, plasticization and modification. *Carbohydrate Polymers, 86*(2), 424-428.

Wu, X., Liu, M., Zhong, X., Liu, G., Wyman, I., Wang, Z., et al. (2017). Smooth Water-Based Antismudge Coatings for Various Substrates. *Acs Sustainable Chemistry & Engineering, 5*(3), 2605-2613.

Xie, F., Yu, L., Su, B., Liu, P., Wang, J., Liu, H., et al. (2009). Rheological properties of starches with different amylose/amylopectin ratios. *Journal of Cereal Science, 49*(3), 371-377.

Xie, F., Halley, P. J., & Avérous, L. (2012). Rheology to understand and optimize processibility, structures and properties of starch polymeric materials. *Progress in Polymer Science, 37*(4), 595-623.

Xie, F., Pollet, E., Halley, P. J., & Avérous, L. (2013). Starch-based nano-biocomposites. *Progress in Polymer Science, 38*(10-11), 1590-1628.

Xie, F., Flanagan, B. M., Li, M., Sangwan, P., Truss, R. W., Halley, P. J., et al. (2014). Characteristics of starch-based films plasticised by glycerol and by the ionic liquid 1-ethyl-3-methylimidazolium acetate: a comparative study. *Carbohydrate Polymers, 111*, 841-848.

Xie, F., Flanagan, B. M., Li, M., Truss, R. W., Halley, P. J., Gidley, M. J., et al. (2015). Characteristics of starch-based films with different amylose contents plasticised by 1-ethyl-3-methylimidazolium acetate. *Carbohydrate Polymers, 122*, 160-168.

Xu, Q., Chen, C., Rosswurm, K., Yao, T., & Janaswamy, S. (2016). A facile route to prepare cellulose-based films. *Carbohydrate Polymers, 149*, 274-281.

Xue, T., Yu, L., Xie, F., Chen, L., & Li, L. (2008). Rheological properties and phase transition of starch under shear stress. *Food Hydrocolloids, 22*(6), 973-978.

Yang, J., Xie, F., Wen, W., Chen, L., Shang, X., & Liu, P. (2016). Understanding the structural features of high-amylose maize starch through hydrothermal treatment. *International Journal of Biological Macromolecules, 84*, 268-274.

Youssef, A. M., & El-Sayed, S. M. (2018). Bionanocomposites materials for food packaging applications: Concepts and future outlook. *Carbohydrate Polymers, 193*, 19-27.

Yu, J., Yang, J., Liu, B., & Ma, X. (2009). Preparation and characterization of glycerol plasticized-pea starch/ZnO–carboxymethylcellulose sodium nanocomposites. *Bioresource Technology, 100*(11), 2832-2841.

Zakrzewska, M. E., Bogel-Łukasik, E., & Bogel-Łukasik, R. (2010). Solubility of carbohydrates in ionic liquids. *Energy & Fuels, 24*(2), 737-745.

Zhang, B., Chen, L., Xie, F., Li, X., Truss, R. W., Halley, P. J., et al. (2015). Understanding the structural disorganization of starch in water-ionic liquid solutions. *Physical Chemistry Chemical Physics, 17*(21), 13860-13871.

Zhang, B., Xie, F., Zhang, T., Chen, L., Li, X., Truss, R. W., et al. (2016). Different characteristic effects of ageing on starch-based films plasticised by 1-ethyl-3-methylimidazolium acetate and by glycerol. *Carbohydrate Polymers, 146*, 67-79.

Zhang, B., Xie, F., Shamshina, J. L., Rogers, R. D., McNally, T., Wang, D. K., et al. (2017). Facile Preparation of Starch-Based Electroconductive Films with Ionic Liquid. *Acs Sustainable Chemistry & Engineering, 5*(6), 5457-5467.

Zhang, K., Cheng, F., Lin, Y., Zhou, M., & Zhu, P.-x. (2018). Effect of hyperbranched poly(trimellitic glyceride) with different molecular weight on starch plasticization and compatibility with polyester. *Carbohydrate Polymers, 195*, 107-113.

Zhang, L.-M., & Chen, D.-Q. (2002). An investigation of adsorption of lead(II) and copper(II) ions by water-insoluble starch graft copolymers. *Colloids and Surfaces A: Physicochemical and Engineering Aspects, 205*(3), 231-236.

Zhong, X.-M., Wyman, I., Yang, H., Wang, J.-B., & Wu, X. (2016). Preparation of robust anti-smudge coatings via electrophoretic deposition. *Chemical Engineering Journal, 302*, 744-751.

Zhu, S., Wu, Y., Chen, Q., Yu, Z., Wang, C., Jin, S., et al. (2006). Dissolution of cellulose with ionic liquids and its application: A mini-review. *Green Chemistry, 8*(4), 325-327.

Zuo, Y., Gu, J., Tan, H., & Zhang, Y. (2015). Thermoplastic starch prepared with different plasticizers: Relation between degree of plasticization and properties. *Journal of Wuhan University of Technology-Mater. Sci. Ed., 30*(2), 423-428.